

# Theoretical Consideration on Influences of Cavity or Pillar Shape on Band Structures of Silicon-Based Photonic Crystals

Yoshifumi Ogawa, Issei Tamura, Yasuhisa Omura, and Yukio Iida

**Abstract**—This paper describes physical meanings of various influences of cavity (or pillar) shape and filling factor of dielectric material on band structures in two-dimensional photonic crystals. Influences of circular and rectangular cross-sections of cavity (or pillar) arrays on photonic band structures are considered theoretically, and significant aspects of square and triangular lattices are compared. It is shown that both averaged dielectric constant of the photonic crystal and distribution profile of photon energy play important roles in designing optical properties. For the triangular lattice, especially, it is shown that cavity array with a rectangular cross-section breaks the band structure symmetry. So, we discuss this point from the band structure and address optical properties of lattice with a circular cross-section cavity.

**Index Terms**—Photonic band, SOI, two dimensional, cavity, pillar

## I. INTRODUCTION

The increasing scale of integrated Si devices has given rise to a significant increase in the signal delay time between circuit blocks; the signal delay time is now much longer than the gate delay time of individual devices. It was hoped that this difficulty could be

overcome by an advanced metallization technique that replaces Al-based wires with Cu-based wires and the SiO<sub>2</sub>-based interlayer dielectrics with a low-k dielectric material. However, it is anticipated that the propagation delay time of interconnections will still determine the speed of integrated circuits when the gate length falls under 0.18  $\mu\text{m}$ . This problem may be overcome by setting optical links between circuit blocks in a chip or LSIs to transfer signals. Silicon-based waveguides have been widely studied from the viewpoints of monolith circuits and process compatibility [1]. The designs must allow for problems such as sharp bends, mode dispersion, and specific attenuation.

Against this background, photonic crystal (PC) materials are attracting attention for controlling light wave transmission [2-4]; photonic bandgap (PBG) structures are especially useful in applications where the spatial localization of light waves is required [5]. In a three-dimensional (3-D) PC, we can control the propagation of light waves in all directions. Generally speaking, however, it is very difficult to fabricate 3-D PC structures. Its simpler cousin, 1-D PC, offers significant easier fabrication at the cost of reduced functionality. Recently, the influence of defects in 1-D PC waveguides with periodic air cavities has been demonstrated experimentally and the characteristics of such waveguides have been verified by simulations [6]. However, it has been clarified that design parameters, such as the shape and dimensions of the air cavities, significantly affect the characteristics of the 1-D PC waveguide [7].

On the other hand, a two-dimensional (2-D) photonic crystal has a high potential of light-beam control capability and the 2-D PC has attracted much attention

---

Manuscript received Sep. 1, 2006; revised Jan. 18, 2007.  
Dept. of Electronics, Kansai University, 3-3-35, Yamate-cho, Suita,  
Osaka 564-8680, Japan  
E-mail : omuray@ipcku.kansai-u.ac.jp

[8-21]. Since 2-D photonic crystal has a flexible photonic band structure, the propagation of light wave can be controlled using the 2-D PC [1, 2]. In addition, in some cases, the PC gives a specific restriction to light-wave propagation even out of PBG; super-prism, self-collimation and super-lens are typical phenomena [9-12]. These phenomena suggest higher potential applications of the PC to information processing. So, the 2D PC has been investigated widely. From the point of view of physics-based consideration, the pillar or cavity array with a circular or rectangular cross-section is investigated extensively [13, 14] because pillar shapes influence dispersion relation of light-wave propagation.

In this paper, we categorize aspects of optical properties of the PC consisted of square lattice of triangular lattice with a circular or rectangular cross-section of pillar or cavity. We also address specific feature of the triangular lattice because of break of propagation symmetry.

## II. PERIODIC CAVITY ARRAY

In this paper, we consider two kinds of lattice structures; square lattice and triangular lattice. As well known, these lattices show quite different photonic band structures; perfect band gap is created for triangular lattices. In the following sections, photonic band structures of lattices with air cavity array and pillar array are considered. In the simulations, two-dimensional lattices are assumed. Band structures are calculated by the orthogonal plane wave expansion (OPW) method; the photonic band structures are obtained by solving with 225-plane waves [3].

### 1. Square Lattice

At first, we consider photonic bands of an air cavity array in silicon. A square lattice with air cavities whose cross-sections are circular or rectangular is shown in Fig. 1; the periodic cavity array is assigned in x-y plane. It is assumed that material is uniform along with the z direction. In Fig. 1,  $a$  is the lattice constant,  $r$  is the radius of cavity having a circular cross-section,  $d$  is the width of rectangular cavity. We calculate the

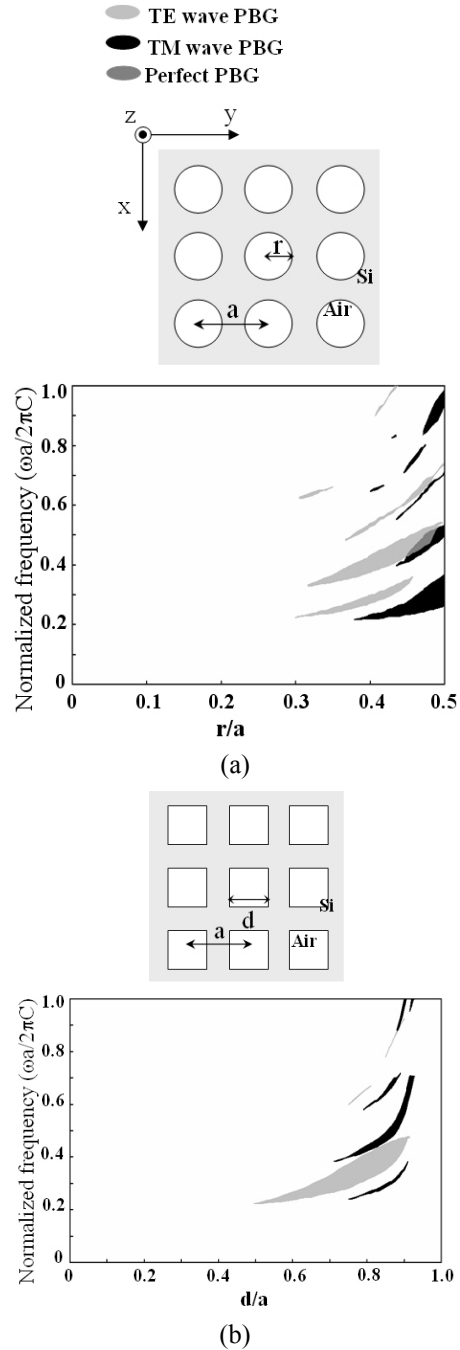


**Fig. 1.** Photonic band gap (PBG) map for various square lattices.: (a) Circular cross-section of cavity (b) Rectangular cross-section of cavity.

dispersion relations of these photonic crystals for various  $r/a$  or  $d/a$  values. Fig. 1(a) shows the photonic band gap (PBG) map for the square lattice in which cross-section of air cavity is circular. The vertical axis shows the normalized frequency  $(\omega a/2\pi c)$ , where  $c$  is the light wave velocity. The horizontal axis shows the circular radius normalized by the lattice constant  $(r/a)$ .

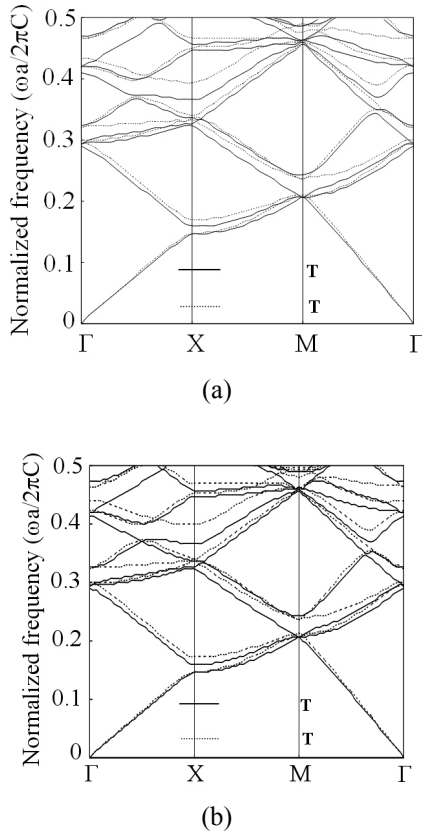
In the photonic band gap map, the gray zone shows the photonic band gap for the TE wave (magnetic field is parallel along with the depth of air cavity); inside the gray zone, the TE wave doesn't propagate regardless of crystal axis. Black zone shows the photonic band gap for the TM wave (electric field is parallel along with the depth of air cavity); inside the black zone, the TM wave doesn't propagate regardless of crystal axis. Dark gray zone shows the perfect photonic band gap in which any light wave mode doesn't propagate. The band gap for the TE wave and that for the TM wave overlap partly as seen in Fig. 1(a).

Fig. 1(b) shows the PBG map for the square lattice in which cross-section of cavity is rectangular. In Fig. 1(b), the horizontal axis shows a width of rectangular cavity normalized by the lattice constant ( $d/a$ ). Comparing features of two photonic band-gap maps, the photonic band gap of TE wave for the lattice with a rectangular cross-section is wider than that for the lattice with a circular cross-section, and the photonic band gap

of TM wave for the lattice with a rectangular cross-section is narrower than that for the lattice with a circular cross-section. The perfect photonic band gap shares a limited zone for the lattice with a circular cross-section (See Fig. 1(a)). Here we define the filling factor ( $f$ ) which denotes the ratio of cavity cross-sectional area to unit cell area;  $f = \pi r^2/a^2$  for the circular cross-section and  $f = d^2/a^2$  for rectangular cross-section. At a small filling factor ( $f$ ), we can see little difference of band structures between these two cavity shapes.

Figs. 2(a) and 2(b) show dispersion relations for the square lattice with a circular cross-section ( $r/a=0.17$  in Fig. 2(a)) and the square lattice with a rectangular cross-section ( $d/a=0.30$  in Fig. 2(b)). The values of  $r/a$  and  $d/a$  are taken such that filling factors of these two lattices are identical to each other ( $f=0.09$ ). Since  $f$  value is so small, the difference of dispersion relations is not notable; the lattice shape does not influence the band structure because of small volume of cavity. We have examined whether the filling factor results in a very slight influence on dispersion relations for  $f < 0.16$ .

Figs. 3(a) and 3(b) show additional dispersion relations for the square lattice with a circular cross-section ( $r/a=0.48$  in Fig. 3(a)) and the square lattice with a rectangular cross-section ( $d/a=0.85$  in Fig. 3(b)). When  $r/a$  and  $d/a$  have a large value, it is obviously seen that the two dispersion relations have distinct differences. Here, to take the same manner as the above, we assumed the ideal filling factor of  $0.72$  in the two square lattices. In Fig. 3(a), we have wide PBG for the TM wave around the normalized frequency ( $\omega a/2\pi c$ ) of 0.3 and the no PBG for the TE wave for the case of square lattice with circular cross-section cavities. In the Fig. 3(b), on the other hand, we have a very narrow PBG for the TM wave and wide PBG for the TE wave for the case of square lattice with rectangular cross-section cavities. In considering the results, there is the well-known general rules of thumb in which a TM-mode PBG is apt to appear in a lattice of effectively-isolated dielectric regions and a TE-mode PBG is apt to appear in a lattice structure of un-isolated dielectric regions [2]. We can understand the mechanism as follows. Since the TE wave has the electric field assigned in x-y plane (see Fig. 1), the electric energy is easily stored in the un-isolated dielectric regions of the



**Fig. 2.** Dispersion relations for various square lattices ( $f=0.09$ ). Solid lines are for TM waves and broken lines are for TE waves. (a) Circular cross-section of cavity ( $r/a=0.17$ ). (b) Rectangular cross-section of cavity ( $d/a=0.30$ ).

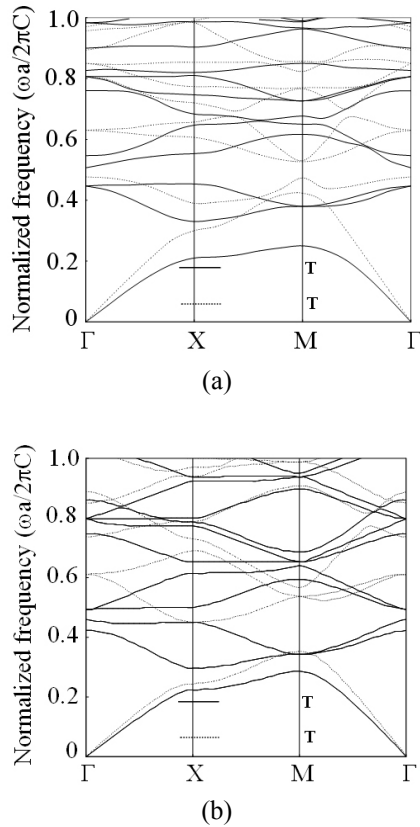
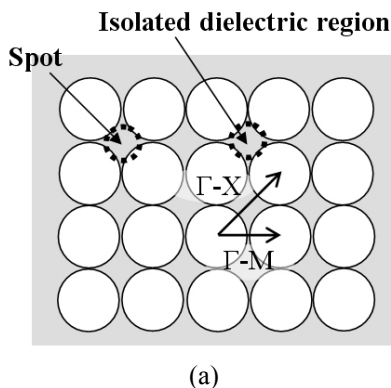
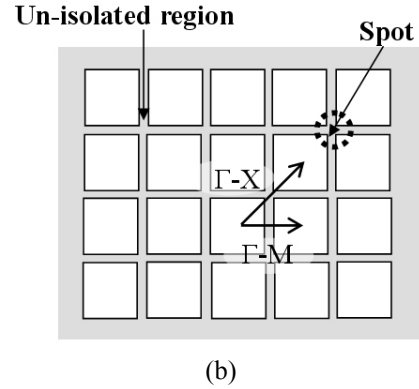


**Fig. 3.** Dispersion relations for various square lattices ( $f=0.72$ ). Solid lines are for TM waves and broken lines are for TE waves. (a) Circular cross-section of cavity ( $r/a=0.48$ ). (b) Rectangular cross-section of cavity ( $d/a=0.85$ ).

lattice. Since the TM wave has the electric field along with  $z$  direction (see Fig. 1), the electric energy is easily stored in the isolated dielectric regions of the lattice. Band gap is created when we have an energy difference between the wave existing stationary in the material with a large averaged refractive index and the wave in a small averaged refractive index, which is realized at the boundaries of corresponding Brillouin zone.



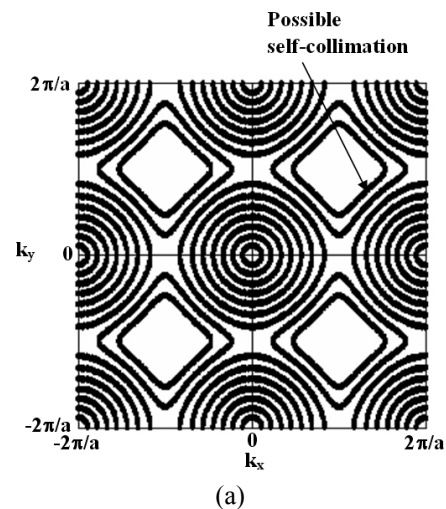
(a)



(b)

**Fig. 4.** Illustrations of PC's having a large filling factor for various square lattices ( $f=0.72$ ). (a) Circular cross-section of cavity. (b) Rectangular cross-section of cavity.

Figs. 4(a) and 4(b) illustrate examples of photonic crystal with a large filling factor. In Fig. 4(a), the lattice with a large cavity of circular cross-section is ready to leave behind isolated dielectric regions, while the lattice with a rectangular cross-section make un-isolated dielectric regions as shown in Fig. 4(b). This difference of structure-dependent aspects of two-different lattices results in the difference of dispersion relations and PBG's shown in Figs. 3(a) and 3(b). In addition, the spot shape (Fig. 4) yields difference between the two dispersion relations. Since the spot is made of Si surrounded with air cavity in silicon-on-insulator (SOI) substrate, most part of light wave energy is stored inside the spot (Si) with a dielectric constant higher than air cavity. The geometrical difference of spot shape brings out the difference of dispersion relations even for the identical filling factor.



(a)

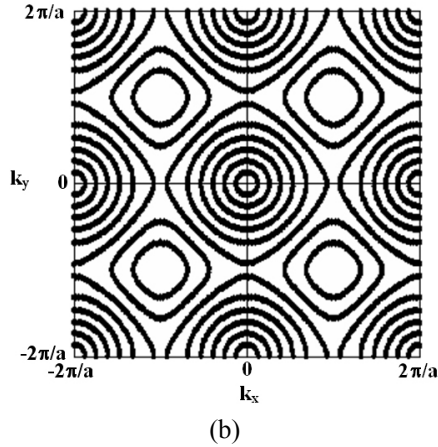


**Fig. 5.** Equi-frequency contours for various square lattices ( $f=0.72$ ). (a) Circular cross-section of cavity ( $r/a=0.48$ ). (b) Rectangular cross-section of cavity ( $d/a=0.85$ ).

Aspects of dispersion relations of different cavity shape appear not only in the frequency range of PBG but also in equi-frequency contours. Equi-frequency contours of TE wave are plotted in Fig. 5; those for the lattice with a circular cross-section ( $r/a=0.48$ ) are shown in Fig. 5(a) and those with a rectangular cross-section ( $d/a=0.85$ ) are shown in Fig. 5(b). Vertical and horizontal axes stand for wave number  $k_x$  and the wave number  $k_y$ , restrictively. Even for the identical filling factor ( $f=0.72$ ), the line shape of equi-frequency contours for different cavity cross-sections shows a

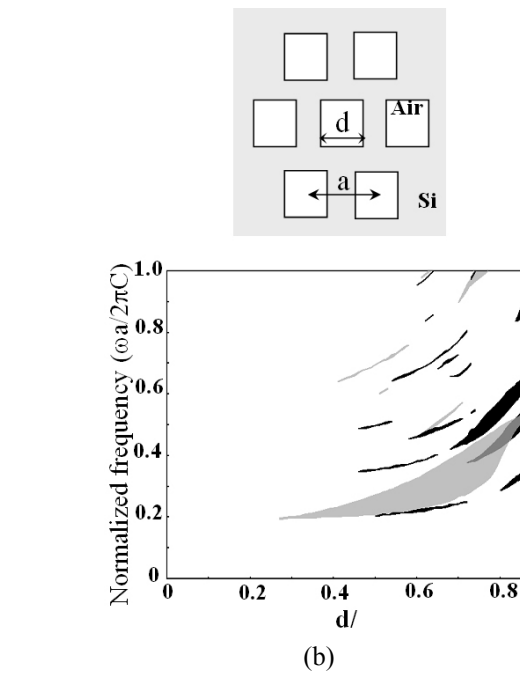
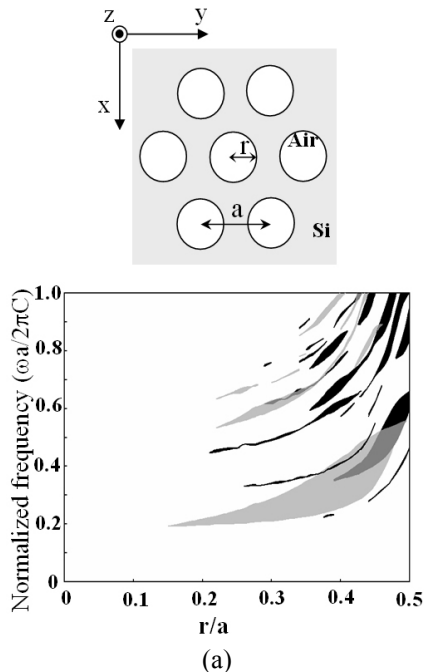


**Fig. 6.** The PBG map for various triangular lattices. (a) Circular cross-section of cavity. (b) Rectangular cross-section of cavity.

somewhat different aspect. It is expected that weak self-collimation of light waves will be observed for the square lattice with a circular cross-section of cavity (see Fig. 5(a)), but not for the lattice with a rectangular cross-section of cavity (see Fig. 5(b)).

## 2. Triangular Lattice

A triangular lattice with cavities of a circular or rectangular cross-section is shown in Fig. 6. Parameter notations ( $a$ ,  $r$  and  $d$ ) are the same as those used in Fig. 1. We calculated dispersion relations of these photonic crystals for various  $r/a$  or  $d/a$  values. Fig. 6(a) shows the PBG map for the triangular lattice with cavities of a circular cross-section. The vertical axis shows the normalized frequency ( $\omega a/2\pi c$ ). The horizontal axis shows the circular radius normalized by the lattice constant ( $r/a$ ). As shown in Fig. 6(a), the circular cross-section cavity makes the wide TE-wave PBG, the TM-wave PBG is narrower than the TE-wave PBG. Fig. 6(b) shows the PBG map for the triangular lattice with a rectangular cross-section cavity. Vertical and horizontal axes stand for the normalized frequency ( $\omega a/2\pi c$ ) and the rectangular cavity width normalized by

the lattice constant ( $\mathbf{d}/\mathbf{a}$ ). On comparing features of two PBG maps, it is seen that the TE-wave PBG for the lattice with a circular cross-section cavity has features similar to those for the lattice with a rectangular cross-section cavity; the TM-wave PBG for the lattice with a rectangular cross-section cavity is separated into two regions and the polarization-independent PBG for the lattice with a circular cross-section cavity is wider than that for the lattice with a rectangular cross-section cavity. However, just like the square lattice, we can see a negligible difference of band structures between lattices with two-different cavity shapes for a small filling factor.

Now, we address band-structure symmetry in a triangular lattice with cavities of a rectangular cross-section. The real-space triangular lattice is shown in Fig. 7(a) and the triangular lattice in the corresponding reciprocal space is shown in Fig. 7(b). In Fig. 7(a), material geometry along the vector  $\vec{a}$  is different from that along the vector  $\vec{b}$  because cavity cross-section is rectangular cross-section, which is a significant aspect of triangular lattice with rectangular cavities. As a result, optical properties at points  $K'$  and  $M'$  in the first Brillouin zone are not equal to those at points  $K$  and  $M$  of the first Brillouin zone as shown in Fig. 7(b). A triangular lattice with cavities of a rectangular cross-section breaks band structure symmetry, but it still has the band structure symmetry of 120 degrees. On the other hand, a triangular lattice with cavities of a circular cross-section has the band structure symmetry of 60 degrees.

As described for a square lattice, when  $\mathbf{r}/\mathbf{a}$  or  $\mathbf{d}/\mathbf{a}$  has a small value, both dispersion relations for a triangular lattice with cavities of a rectangular cross-section and those for a triangular lattice with cavities of circular cross-section have little difference. When  $\mathbf{r}/\mathbf{a}$  or  $\mathbf{d}/\mathbf{a}$  has a small value, difference of optical properties between points  $K'$  and  $M'$  of the first Brillouin zone and points  $K$  and  $M$  of the first Brillouin zone is not significant for a triangular lattice with cavities of rectangular cross-section.

When  $\mathbf{r}/\mathbf{a}$  or  $\mathbf{d}/\mathbf{a}$  has a large value, two dispersion relations have somewhat different aspect. Figs. 8(a) and 8(b) show calculated dispersion relations for the lattice with cavities of a circular cross-section ( $\mathbf{r}/\mathbf{a}=0.48$ ) and for the lattice with cavities of a rectangular

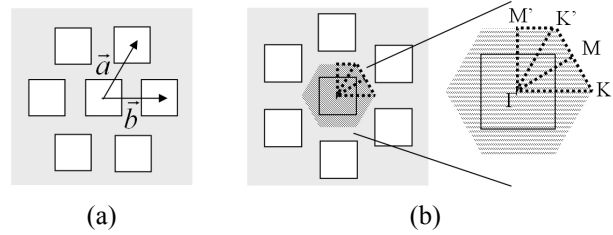


**Fig. 7.** Illustrations of triangular lattice with a rectangular cross-section of cavity. (a) Lattice illustrated in a real space. (b) Reciprocal lattice and Brillouin zone.

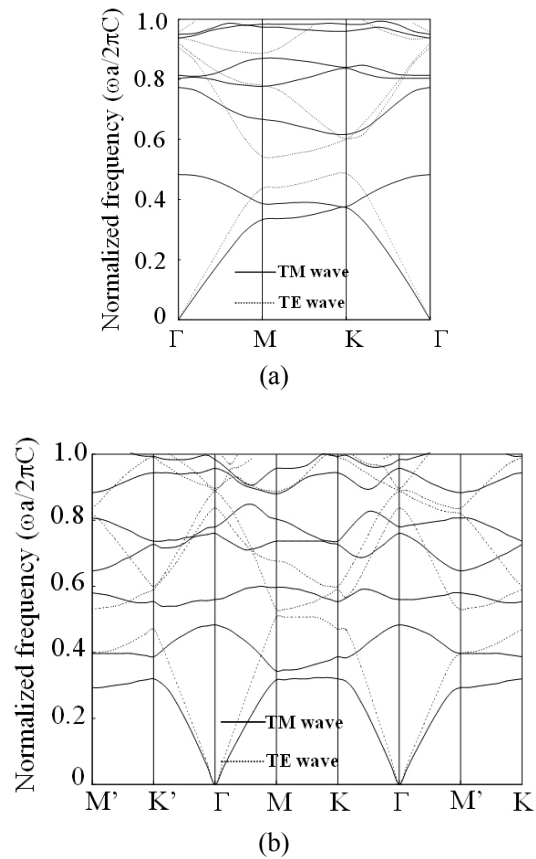


**Fig. 8.** Dispersion relations for various triangular lattices ( $f=0.83$ ). Solid lines are for TM waves and broken lines are for TE waves. (a) Circular cross-section of cavity ( $\mathbf{r}/\mathbf{a}=0.48$ ). (b) Rectangular cross-section of cavity ( $\mathbf{d}/\mathbf{a}=0.85$ ).

cross-section ( $\mathbf{d}/\mathbf{a}=0.85$ ), respectively. In Fig. 8, the filling factors of the two lattices are identical to each other ( $f=0.83$ ); these two dispersion relations have many different features. In Fig. 8(b), the TE-wave PBG along the  $M$  direction of the first Brillouin zone is narrow because of a rectangular cross-section cavity. Figs. 9(a) and 9(b) illustrate two-different PC structures with a large filling factor. In Fig. 9(a), we can see isolated Si spots surrounded by air cavities independently of

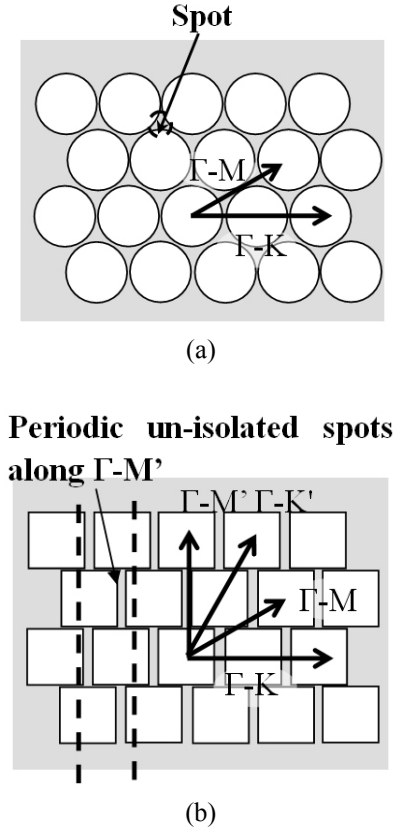


**Fig. 9.** Illustrations of PC's having a large filling factor for various triangular lattices. (a) Circular cross-section of cavity. (b) Rectangular cross-section of cavity.

crystal axis. In Fig. 9(b), there is no un-isolated spot along the  $\Gamma-M$  direction. So, since the TE-wave PBG is easily created for un-isolated spots, the TE-wave band gap along the  $\Gamma-M$  direction is narrow. In addition, the dispersion relation along the  $\Gamma-M$  direction is different from that along the  $\Gamma-M'$  direction as shown in Fig. 8(b). In Fig. 9(b), the  $\Gamma-M'$  direction has periodic-un-isolated spots; the TE-wave band gap along the  $\Gamma-M'$  direction is wider than the TE-wave band gap along of the  $\Gamma-M$  direction. The wide perfect PBG exist for a circular cross-section cavity (see Fig. 8(a)), while the narrow perfect PBG exists for a rectangular cross-section cavity (see Fig. 8(b)). This is caused by the difference of spot shape.

### III. PERIODIC SILICON PILLAR ARRAY

Finally we discuss optical properties of lattices with a Si pillar array. The PC structures with Si pillar array are shown in Fig. 10; Figs. 10 (a) and 10(b) are composed of

square lattice and Figs. 10(c) and (d) are composed of triangular lattice and Figs. 10(c) and (d) are composed of triangular lattice; Figs. 10(a) and 10(c) show PC's with a circular cross-section pillar and Figs. 10(b) and 10(d) show PC's with a rectangular cross-section pillar. Parameter values of  $a$ ,  $r$  and  $d$  are the same as those used in Fig. 1 for square lattices and Fig. 6 for triangular lattices. Fig. 11 shows the PBG maps for a square lattice with a circular cross-section pillar as a typical simulation result. The vertical axis shows the normalized frequency ( $\omega a/2\pi c$ ). The transverse axis shows the circular radius normalized by the lattice constant ( $r/a$ ). For the Si pillar array, we can see only isolated Si regions, not un-isolated Si regions; this depends on filling factor ( $f$ ). TM wave has a wide PBG, while TE wave has a narrow PBG. Since dielectric spots are made of air with a lower dielectric constant, the light wave energy is stored in Si pillars with a higher dielectric constant. In the present cases, the effective permittivity of PC region is ruled by silicon pillars. This suggests that simulation results for band structures of PC structures shown in Fig. 10 are almost identical to each other regardless of pillar shapes; actually simulation results show availability of this prediction (not shown here).

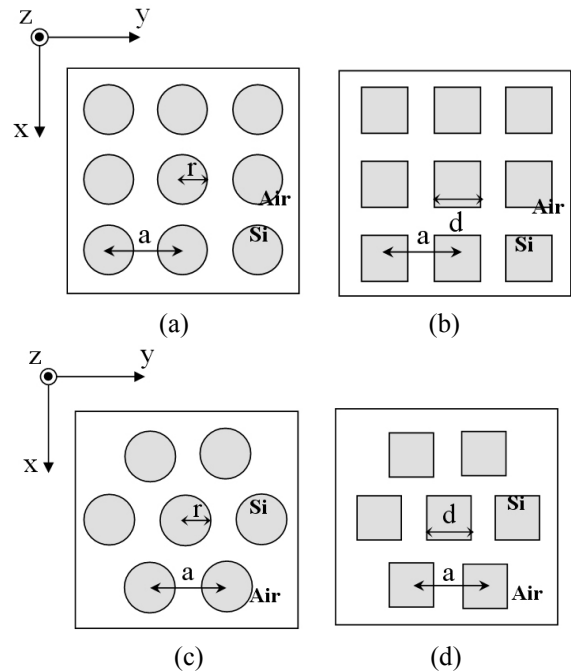


**Fig. 10.** Illustrations of PC's for various lattice structures. (a) Square lattice with pillars of a circular cross-section. (b) Square lattice with pillars of a rectangular cross-section. (c) Triangular lattice with pillars of a circular cross-section. (d) Triangular lattice with pillars of a rectangular cross-section.

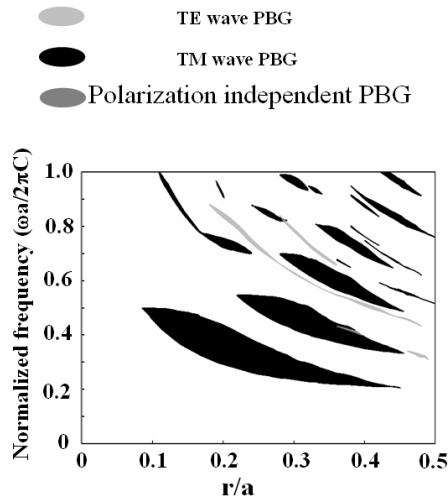


Fig. 11. PBG maps for various lattices shown in Fig. 10(a). Square lattice with pillars of a circular cross-section is assumed.

#### IV. CONCLUSIONS

We investigated how the optical band structure of PC depends on lattice array structure (square lattice or triangular lattice) and cross-sectional shape of lattice point (circular or triangular shape). Band structures of PC's are categorized from the point of view of PBG map. In lattices with the air cavity array, we can see slight difference of dispersion relations independently of cavity shape when the filling factor is small. However, when the filling factor is large, it is clearly shown that those two dispersion relations have somewhat different aspects; in other words, the cross-section of lattice point modulates the band structure. Difference of optical property of lattices with cavity or pillar of a circular or rectangular cross-section results not only in PBG aspect, but also in equi-frequency contours. For the triangular lattice, it is shown that the rectangular cross-section of lattice point breaks the band structure symmetry. For lattices with Si pillar array, we can see a slight difference of band structure between two-different pillar shapes because spots are made of air.

#### ACKNOWLEDGMENTS

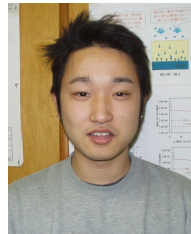
This study is financially supported by Kansai University Grant-in-Aid (Joint Research) 2003.

#### REFERENCES

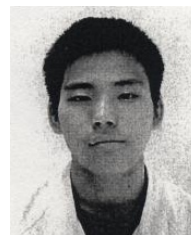
- [1] R. A. Soref and J. P. Lorenzo, "All-Silicon Active and Passive Guided-Wave Components for  $\lambda = 1.3$  and  $1.6 \mu\text{m}$ ," *IEEE J. Quantum Electronics*, vol. QE-22, no. 6, pp. 873-879, 1986.
- [2] J. D. Joannopoulos, R. D. Meade, and J. N. Winn, "Photonic Crystals -Molding the Flow of Light," *Princeton University Press*, Princeton, NJ, 1995.
- [3] K. Sakoda, "Optical Properties of Photonic crystals", *Springer*, New York, 2001.
- [4] E. Yablonovitch, "Inhibited Spontaneous Emission in Solid-State Physics and Electronics," *Phys. Rev. Lett.*, vol. 58, pp. 2059-2062, 1987.
- [5] A. Mekis, J. C. Chen, I. Kurland, S. Fan, P. R. Villeneuve, and J. D. Joannopoulos, "High Transmission Through Sharp Bends in Photonic Crystal Waveguides," *Phys. Rev. Lett.*, vol. 77, pp. 3787-3790, 1996.
- [6] J. S. Foresi, P. R. Villeneuve, J. Ferrera, E. R. Thoen, G. Steinmeyer, S. Fan, J. D. Joannopoulos, L. C. Kimerling, H. I. Smith and E. P. Ippen, "Photonic-Bandgap Microcavities in Optical Waveguides," *Nature*, vol. 390, pp. 143-145, 1997.
- [7] T. Kinoshita, A. Shimizu, Y. Iida and Y. Omura, "Design Sensitivity in Quasi-One-Dimensional Silicon-Based Photonic Crystalline Waveguides," *J. Semicond. Tech. and Sci.*, vol. 3, pp. 55-61, 2003.
- [8] A. Polman, P. Wiltzius, T.A.Birks, E.Chow, V.L.Colvin, J.G.Fleming, J.C.Knight, S.Lin, S.Noda, P.S.J.Russell, J.Schilling, W.L.vos, A.J.Turberfield, R.B.Wehrspohn, "Materials Science Aspects of Photonic Crystals," *MRS BULLETIN*, No. 8, pp. 608-610, 2001.
- [9] X. Yu and S. Fan, "Bends and Splitters for Self-Collimated Beams in Photonic Crystals," *Appl. Phys. Lett.*, vol. 83, no. 16, pp. 3251-3253, 2003.
- [10] H. Kosada, T. Kawashima, A. Tomita, M. Notomi, T. Tamamura, T. Sato, and S. Kawakami, "Superprism Phenomena in Photonic Crystals," *Phys. Rev. B*, vol. 58, no. 16, pp. 10096-10099, 1998.

- [11] C. Luo, S. G. Johnson, and J. D. Joannopoulos, "Subwavelength Imaging in Photonic Crystals," *Phys. Rev. B*, vol. 68, pp. 045115-1-15, 2003.
- [12] A. I. Cabuz, E. Centeno, and D. Cassagne, "Superprism Effect in Bidimensional Rectangular Photonic Crystals," *Appl. Phys. Lett.*, vol. 84, no. 12, pp. 2031-2033, 2004.
- [13] N. Susa, "Large Absolute and Polarization-Independent Photonic Band Gaps for various Lattice Structures and Rod Shapes," *J. Appl. Phys.*, vol. 91, no. 6, pp. 3501-3510, 2002.
- [14] R. Wang, X. H. Wang, B. Y. Gu, and G. Z. Yang, "Effects of Shapes and Orientations of Scatterers and Lattice Symmetries on The Photonic Band Gap in Two-Dimensional Photonic Crystals," *J. Appl. Phys.*, vol. 90, no. 9, pp. 4307-4313, 2001.
- [15] C. Y. Hong, I. Drikis, S. Y. Yang, H. E. Horng, and H. C. Yang, "Slab-Thickness Dependent Band Gap Size of Two-Dimensional Photonic Crystals with Triangular-Arrayed Dielectric or Magnetic Rods," *J. Appl. Phys.*, vol. 94, no. 4, pp. 2188-2191, 2003.
- [16] Y. Akahane, T. Asano, B. S. Song, AND S. Noda, "Investigation of High-Q Channel Drop Filters Using Donor-Type Defects in Two-Dimensional Photonic Crystal Slabs," *Appl. Phys. Lett.*, vol. 83, no. 8, pp. 1512-1514, 2003.
- [17] L. L. Lin, Z. Y. Li, and K. M. Ho, "Lattice Symmetry Applied in Transfer-Matrix Methods for Photonic Crystals," *J. Appl. Phys.*, vol. 94, no. 2, pp. 811-821, 2003.
- [18] R. L. Chern, C. C. Chang, C. C. Chang, and R. R. Hwang, "Large Full Band Gaps for Photonic Crystals in Two Dimensions Computed by an Inverse Method with Multigrid Acceleration," *Phys. Rev. E*, vol. 68, pp. 026704-1-5, 2003.
- [19] J. M. Hickmann, D. Solli, C.F. McCormick, R. Plambeck, and R.Y. Chiao, "Microwave Measurements of The Photonic Band Gap in a Two-Dimensional Photonic Crystal Slab," *J. Appl. Phys.*, vol. 92, no. 11, pp. 6918-6920, 2002.
- [20] X. Hu, Y. Shen, X. Liu, R. Fu, and J. Zi, "Superlensing Effect in Liquid Surface Waves," *Phys. Rev. E*, vol. 69, pp. 030201-1-4, 2004.
- [21] Y. Iida, Y. Omura, Y. Ogawa, T. Kinoshita, and M. Tsuji, "Ring Resonator with Sharp U-Turns Using

a SOI-Based Photonic Crystal Waveguide with Normal Single-Missing-Hole-Line Defect," *Proc. of SPIE*, vol. 5277, pp. 206-214, 2003.



**Yoshifumi Ogawa** was born in 1979 in Chiba Pref., Japan, and received the B. S. degree and M. S. degree in Electronics from Kansai University in 2003, and in 2005, respectively. He is presently with CANON Corporation, Japan.



**Issei Tamura** was born in 1982 in Osaka Pref., Japan, and received the B. S. degree in Electronics from Kansai University in 2004.



**Yasuhisa Omura** received the M. S. degree in applied science in 1975 and the Ph. D. degree in electronics in 1984, both from Kyushu University, Japan. He joined the Musashino Electrical Communications Laboratories, NTT, Tokyo, Japan in 1975. He worked on short-channel CMOS/SIMOX design, LSI processing, and SOI device modeling. In NTT, he contributed to trial demonstrations of CMOS/SIMOX SRAM on the device design and fabrication processing. He moved his position from NTT Atsugi R&D Center to Kansai University, Osaka Prefecture, as a professor after April in 1997, and he is presently working on device physics of ultimately miniaturized MOSFET/SOI, modeling for MOS device design, fluctuation physics and development of silicon photonic devices. He has published 110 regular papers and 110 conference proceedings. He is one of coauthors having published "Device and Circuit Cryogenic Operation for Low Temperature Electronics." (Kluwer Academic Publishers, 2001) and "Fully-Depleted SOI CMOS Circuits and Technology for Ultralow-Power Applications" (Springer, 2006). He has invented various SOI devices-for example-the lateral unidirectional bipolar-type insulated-gate transistor (Lubistor), the high-gain

cross-current tetrode (HXT) MOS device, and tunneling-barrier junction (TBJ) SOI MOSFET using SIMOX technology. He has patents for Lubistor in Japan, U.S.A., Canada, United Kingdom, France, Germany, Netherlands, Italy, and Korea. He has 30 patents in Japan and several patents in U.S.A. for SIMOX device technology. He was honored with the Annual Young Researcher Award in 1981 from IEICE, Japan. He has worked on ultra-thin MOSFET/SIMOX device technology over 20 years. Last decade, he demonstrated 0.1-  $\mu$ m-gate CMOS/SIMOX devices with a long lifetime in 1991 IEEE IEDM and 1992 Int. Conf. on Solid State Devices and Materials (SSDM). He also demonstrated mesoscopic transport characteristics of 50-nm-channel SOI MOSFETs with 2- or 6-nm-thick silicon film in order to indicate perspectives of future SOI devices in 1997. He served the Technical Committee of IEEE Int. SOI Conf. from 1997 to 1998, and now serves the Program Committee of Int. Symp. on VLSI Technology from 1997 to 2006. In addition, he serves the Program Committee of Int. Workshop on Low-Temperature Electronics (in Europe) from 1998 to now. From 2007, he shares the Vice Chairperson of IEEE Kansai Chapter. Dr. Omura is a regular member of the Japan Society of Applied Physics (JSAP), the Physical Society of Japan, the Electrochemical Society, a senior member of the Institute of Electrical and Electronics Engineers (IEEE) and a regular member of the Institute of Electronics, Information and Communication Engineers (IEICE).



**Yukio Iida** received the B.E., M.E. and D. Eng. degrees from Kansai University, Osaka, Japan, in 1970, 1972 and 1983, respectively. Since 1979 he has been working at the Department of Electronics, Faculty of Engineering, Kansai University.

He was a Research Assistant in 1979, a Lecturer and an Associate Professor. Since 1998 he has been a Professor. He has been engaged in the research of microwave electron tube (Osaka-tube and Gyrotron), wireless blasting system by microwave power, injection locking and multiple oscillation in Gunn, IMPATT and LASER diodes, Spatial network method, FDTD method, electromagnetic field simulation, and silicon microphotonics application including photonic crystal. Dr. Iida is a member of the Institute of Electronics, Information and Communication Engineers (IEICE), Japan, and the IEEE Microwave Theory and Techniques society (IEEE MTT-S).